JCTC Journal of Chemical Theory and Computation

Article

pubs.acs.org/JCTC

Multiconfiguration Pair-Density Functional Theory

Giovanni Li Manni,[†,§] Rebecca K. Carlson,[†,§] Sijie Luo,[†,§] Dongxia Ma,[†,§] Jeppe Olsen,[‡] Donald G. Truhlar,*[,†] and Laura Gagliardi*[,†]

[†]Department of Chemistry, Supercomputing Institute, and Chemical Theory Center, University of Minnesota, Minneapolis, Minnesota 55455, United States

[‡]Department of Chemistry, Aarhus University, Langelandsgade 140, DK-8000, Aarhus C, Denmark

Supporting Information

ABSTRACT: We present a new theoretical framework, called Multiconfiguration Pair-Density Functional Theory (MC-PDFT), which combines multiconfigurational wave functions with a generalization of density functional theory (DFT). A multiconfigurational self-consistent-field (MCSCF) wave function with correct spin and space symmetry is used to compute the total electronic density, its gradient, the on-top pair density, and the kinetic and Coulomb contributions to the total electronic energy. We then use a functional of the total density, its gradient, and the on-top pair density to calculate the remaining part of the energy, which we call the on-top-density-functional energy in contrast to the exchange-correlation energy of Kohn–Sham DFT. Because the on-top pair density is an element of the two-particle density matrix, this goes beyond the Hohenberg–Kohn theorem that refers only to the one-particle density. To illustrate the theory, we obtain first approximations to the required new type of density functionals by translating conventional density functionals of the spin densities using a simple prescription, and we perform post-SCF density functional calculations using the total density, density gradient, and on-top pair density from the MCSCF calculations. Double counting of dynamic correlation or exchange does not occur because the MCSCF energy is not used. The theory is illustrated by applications to the bond energies and potential energy curves of H_2, N_2, F_2, CaO, Cr_2, and NiCl and the electronic excitation energies of Be, C, N, N^+, O, O^+, Sc^+, Mn, Co, Mo, Ru, N_2, HCHO, C_4H_6, *c*-C_5H_6, and pyrazine. The method presented has a computational cost and scaling similar to MCSCF, but a quantitative accuracy, even with the present first approximations to the new types of density functionals, that is comparable to much more expensive multireference perturbation theory methods.

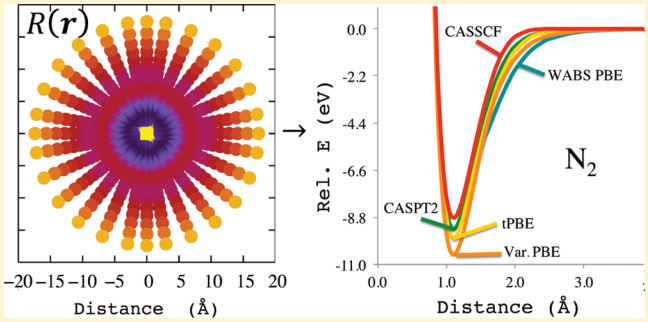

1. INTRODUCTION

In Kohn–Sham Density Functional Theory, KS-DFT,[1] as extended to spin-polarized electronic systems,[2,3] the electronic energy is expressed as a functional of the electron spin densities (in the local-spin-density approximation, LSDA) and their gradients (in the generalized gradient approximation, GGA), as well as possibly as a functional of orbital-dependent quantities such as exchange energy density or kinetic energy density. The dependence on these quantities, as opposed to a dependence on the full two-particle density matrix,[4] makes the method computationally simpler and more affordable than wave function theory (WFT).[5]

A key concern in the present article is the treatment of inherently multiconfigurational systems, that is, systems whose electronic structure cannot be described to a good approximation by only a single way of distributing the electrons in the orbitals of a Slater determinant. Such systems are usually labeled as "strongly correlated" systems or "multireference" systems, where the latter reminds us that a converged treatment by most WFT methods requires a multiconfiguration reference state or zero-order wave function. In WFT, the special types of errors in the energy that arise from using a single-reference treatment of an inherently multiconfigurational system are called "static," "nondynamical," "near-degeneracy," or "left–right" correlation energy.[6−8] Examples of inherently multiconfigurational systems include many transition metal atoms and molecules and solids containing them, partially broken bonds, most excited states of molecules, and some transition states.

In KS-DFT,[1−3] the spin densities are represented by a single Slater determinant, and the spin–orbitals of this determinant are used to evaluate the kinetic energy of the noninteracting electron system with the same density as the real system. The correction to the kinetic energy, the exchange energy, and the correlation energy are then represented by a functional of the spin densities. This functional, called the exchange–correlation functional, is so complicated it will probably never be known exactly.[9] In order to obtain correct energetics, a determinant that is not a spin eigenfunction and has the wrong symmetry may be necessary.[4]

Received: April 5, 2014
Published: July 21, 2014

   dx.doi.org/10.1021/ct500483t | J. Chem. Theory Comput. 2014, 10, 3669−3680

Nevertheless, one must be careful: not all broken symmetry solutions are permissible. Because the true density must respect, e.g., some spatial symmetries, the exact KS theory must only lead to solutions whose total density preserves the appropriate symmetries of the density. Note, however, that producing a density with the correct symmetry is generally less of a constraint on a Slater determinant than producing a wave function with the correct symmetry. Notice also that, in a different approach, it has been proposed to generate true spin-density functionals based on a size-extensive construction of self-interaction correction orbitals.[10]

Moreover, even if a system is inherently multiconfigurational, KS-DFT with the exact functional is exact, even with the single-configuration representation of the density, but the accuracy is typically low with existing functionals.[11−13] Furthermore, it is not always clear which of the nearly degenerate states is being approximated, leading to the development of strategies for interpreting broken-symmetry solutions.[14−21] Therefore, one of the unmet challenges for DFT is the proper treatment of multireference systems and, more generally, the treatment of nearly degenerate states by enforcing their spatial and spin symmetries. Multiconfiguration self-consistent-field (MCSCF) methods, such as the complete active space self-consistent field (CASSCF)[22] method, on the other hand, are able to treat near-degeneracies with no ambiguity about which state is being approximated, but they do not include dynamic correlation energy, which is essential for a quantitative treatment of chemical properties such as bond energies and electronic excitation energies, nor do they include core−valence correlation, which can also be important. Both of these effects can be added by a post-SCF method, for example, multireference perturbation theory [such as complete-active-space second-order perturbation theory (CASPT2)[23]] or multireference configuration interaction (MRCI)[24] methods, using the MCSCF wave function as a reference, but these methods are limited in their applicability, because of high computational cost, which rises steeply as a function of the increasing size of the system (unfavorable scaling with system size). Modern extensions of these methods allow the use of larger active spaces with the formulation of restricted active space (RAS),[25] generalized active space (GAS), and SplitGAS wave functions[26−28] and with the occupation-restricted-multiple-active-space (ORMAS) SCF method.[29] However, the applicability of methods that add approximations to the full dynamic correlation energy based on these types of reference functions (by multireference perturbation theory, multireference configuration interaction, or multireference coupled cluster theory) is still limited to small- to middle-sized systems. For large systems in which both static and dynamic correlation energy are crucial, a method that allows a description of both types of correlation with affordable computational costs is needed.

Several attempts to combine multiconfigurational WFT with DFT-based methods have been proposed, either based on adding some amount of density functional correlation to a multi-configurational wave function calculation[30−73] or adding some amount of wave function correlation to a density functional calculation. The present paper is concerned with the former. The general goal has been to describe static correlation by the multiconfigurational WFT approach, while dynamic correlation is included by DFT. However, two main problems arise in such treatments. The first problem is the double counting of dynamic electron correlation, since any attempt to include static correlation energy by WFT inevitably involves including some dynamic correlation energy. One can try to eliminate that portion of the dynamic correlation from the exchange-correlation functional, but it is very hard to do this in a systematic and accurate way.[43] The second problem involves the choice of input quantities to be used in the density functionals, since existing functionals are not compatible with spin densities of multi-configurational wave functions or generally with any spin- and space-adapted wave function for which the total spin, S, is smaller than half of the number of the singly occupied orbitals (including single-configuration, multideterminantal wave functions). This has been called the "symmetry dilemma" in the context of KS-DFT,[74] and an analogous symmetry dilemma is well-known in Hartree−Fock theory.[75] The situations are different in that, despite having the wrong symmetry for the Slater determinant, KS-DFT would yield the exactly correct one-particle density if one could use the unknown exact density functional, whereas Hartree−Fock theory does not yield the correct one-particle density when applied to a system with two or more interacting electrons.

In the present article, we propose a way to circumvent both of these difficulties. To eliminate double counting of correlation energy, we calculate only the Coulomb energy and a multi-configurational portion of the kinetic energy from the MCSCF wave function, with the rest of the energy calculated by a density functional. To overcome the symmetry dilemma, following a suggestion of Becke et al.[76] and earlier work by Moscardó and San-Fabián,[77] we express the density functional in terms of the total density ρ and on-top pair density Π, which is defined by[78]

$$\Pi(\mathbf{r}) = \binom{N}{2} \int |\Psi(x_1, x_2, ..., x_N)|^2 \, d\sigma_1 \, d\sigma_2 ... d\sigma_N \, d\mathbf{r}_3 \, d\mathbf{r}_4 ... d\mathbf{r}_N|_{\mathbf{r}_1=\mathbf{r}_2=\mathbf{r}} \tag{1}$$

where σ_i is a spin variable, and $x_i = (\mathbf{r}_i, \sigma_i)$ is a space-spin variable, rather than in terms of the total density and the difference between the spin-up and spin-down densities. The density functional of the new theory will be called the "on-top density functional", to distinguish it from the exchange-correlation functional of KS-DFT; the new theory is called "Multi-configuration Pair-Density Functional Theory" (MC-PDFT). To illustrate the theory, we employ multiconfigurational wave functions of CASSCF-type and first approximations to the required new type of density functionals.

We note that another very promising approach to the combination of wave function theory with DFT is provided by range separation.[38,48−50,62] Range separation is a powerful method for improving DFT, and it has been applied in a variety of ways.[79−86] There is no reason why the present approach could not be combined with range separation in later work, but it is beyond our scope to discuss it further in the present article.

We emphasize that the idea of using the total density and on-top density in DFT is not new. Many others have worked on it, and citations are given at appropriate places in the development below. What is new in this work is that, unlike previous "additive" efforts, where a mixture of the form $E(\mathrm{WF}) + \Delta E(\mathrm{DFT})$ was used, we propose evaluating only the classical Coulomb energy and an approximation to the kinetic energy from the reference multiconfiguration "wave function" and evaluating all the rest of the energy from a density functional, called an on-top density functional, in terms of the total density ρ and on-top pair density Π, and we suggest a simple but general way to develop this kind of density functional from Kohn−Sham exchange-correlation functionals that depend only on up-spin and down-spin densities and their gradients. This eliminates all double counting of

correlation energy, and it provides a framework in which better on-top density functionals can be developed. To our knowledge, this has not been attempted previously. At this point, we should also mention some recent work by Garza et al., who proposed to describe electronic correlation without double counting via a combination of spin-projected Hartree−Fock and density functional theories.[87,88]

2. THEORY

2.1. MC-PDFT Equations. We assume the Born−Oppenheimer approximation, and we consider the fixed-nucleus energy E. For a multiconfiguration electronic wave function and a spin-free, nonrelativistic Hamiltonian, the WFT energy, obtained as the expectation value of the Hamiltonian operator, is given by

$$E = V_{\mathrm{nn}} + \sum_{pq} h_{pq} D_{pq} + \frac{1}{2} \sum_{pqrs} g_{pqrs} d_{pqrs} \tag{2}$$

where V_{nn} is the sum of the nucleus−nucleus repulsions, the indices p, q, r, and s refer to generic orbitals, h_{pq} and g_{pqrs} are, respectively, the one-electron and two-electron integrals, and D_{pq} and d_{pqrs} are, respectively, the one- and two-body electronic density matrices.

In the CASSCF method, a complete CI expansion in space and spin symmetry-adapted CSFs is generated by all possible excitations within an active space. One set of orbitals, called the inactive orbitals, is doubly occupied in all configurations. This allows the simplification of the energy expression to

$$E = V_{\mathrm{nn}} + 2\sum_{i} h_{ii} + \sum_{ij} (2g_{iijj} - g_{ijij}) + \sum_{vw} h_{vw} D_{vw} + \sum_{ivw} (2g_{iivw} - g_{ivwi}) D_{vw} + \frac{1}{2} \sum_{vwxy} g_{vwxy} d_{vwxy} \tag{3}$$

where indices i and j denote inactive orbitals, and v, w, x, and y denote active orbitals.

In contrast to the WFT expression, the new MC-PDFT method calculates the energy by

$$E = V_{\mathrm{nn}} + \langle \Psi | T + V_{\mathrm{ne}} | \Psi \rangle + V_{\mathrm{C}}[\rho] + E_{\mathrm{ot}}[\rho, \Pi] \tag{4}$$

where $|\Psi\rangle$ is the multiconfigurational MC wave function, T is the kinetic energy operator, V_{ne} is the electron−nuclear interaction, and $V_{\mathrm{C}}[\rho]$ and $E_{\mathrm{ot}}[\rho,\Pi]$ are the electronic Coulomb energy and the on-top electronic density functional, respectively. This energy may be written in terms of the one-electron density matrix and the on-top density functional as

$$E = V_{\mathrm{nn}} + \sum_{pq} h_{pq} D_{pq} + \frac{1}{2} \sum_{pqrs} g_{pqrs} D_{pq} D_{rs} + E_{\mathrm{ot}}[\rho, \Pi] \tag{5}$$

When we recognize that some orbitals are doubly occupied in all CSFs, this becomes

$$E = V_{\mathrm{nn}} + 2\sum_{i} h_{ij} + 2\sum_{ij} g_{iijj} + \sum_{vw} h_{vw} D_{vw} + 2\sum_{ivw} g_{iivw} D_{vw} + \frac{1}{2} \sum_{vwxy} g_{vwxy} D_{vw} D_{xy} + E_{\mathrm{ot}}[\rho, \Pi] \tag{6}$$

With respect to the WFT energy expression, the two-electron contribution has been replaced by a Coulomb term involving the product of one-particle density matrices and an on-top density functional term.

The generalization to include scalar relativistic effects by using the Douglas−Kroll Hamiltonian[89,90] is straightforward; it simply involves changing the definition of the one-electron terms.[91]

2.2. Pair-Density Functionals. Next, we discuss the choice of on-top density functional. If one approximates an exchange-correlation functional using only local densities and their gradients, an exchange-correlation functional for a spin-polarized system can be written as a functional of the total density ρ, the spin magnetization density m (which may also be called the net spin density), and the magnitudes, $\rho' \equiv |\nabla\rho|$ and $m' \equiv |\nabla m|$, of their gradients, where

$$\rho(\mathbf{r}) = \rho_{\alpha}(\mathbf{r}) + \rho_{\beta}(\mathbf{r}) \tag{7}$$

and

$$m(\mathbf{r}) = \rho_{\alpha}(\mathbf{r}) - \rho_{\beta}(\mathbf{r}) \tag{8}$$

ρ_{α} is the density of majority-spin electrons, and ρ_{β} is the density of minority-spin electrons at a point $\mathbf{r}$. As previously described,[74,76] the exchange-correlation functionals defined in terms of the net spin density give reasonable energies with broken-symmetry Slater determinants in spin-polarized Kohn−Sham theory, but the net spin densities are not appropriate variables for density functionals if the correct spin symmetry is imposed.

Moscardo and San-Fabián[77] discussed using the on-top density of a multiconfiguration wave function to motivate functional forms for including electron correlation in density functionals of the spin densities. Becke et al.[76] discussed changing the independent variables of density functional approximations from ρ and m to ρ and Π. For a single-determinant wave function, m can be related to Π and ρ by the relation[76]

$$m(\mathbf{r}) = \rho(\mathbf{r})[1 - R(\mathbf{r})]^{1/2} \tag{9}$$

where

$$R(\mathbf{r}) = \frac{4\Pi(\mathbf{r})}{\rho(\mathbf{r})^2} \tag{10}$$

with $R \leq 1$ at all points in space. However, for multiconfiguration wave functions, eq 9 is not true, and R can be larger than unity. Later, Perdew et al.[74,92] discussed the use of the ρ and Π variables for interpreting the symmetry dilemma, and Miehlich et al.,[31] McDouall,[40] and Gusarov et al.[42] proposed using functionals of the density and the pair density to recover the difference between the full correlation energy and the MCSCF correlation energy. Tsuchimmochi et al.[93] proposed using a density functional defined in terms of ρ and Π in conjunction with another WFT method, namely constrained-pairing mean-field theory. Here we use ρ and Π to define the on-top density functional for MC-PDFT.

Ultimately, we must develop new on-top density functionals specifically for use with MC-PDFT. As a first step, we simply "translate" previously developed exchange-correlation functionals of spin densities. In particular, given $E_{\mathrm{xc}}(\rho,m,\rho',m')$, we write the following translation prescription:

$$E_{ot}[\rho(\mathbf{r}),\Pi(\mathbf{r})] = E_{xc}\left(\rho(\mathbf{r}),\begin{cases}\rho(\mathbf{r})(1-R)^{1/2} & \text{if } R\le 1\\ 0 & \text{if } R>1\end{cases},\rho'(\mathbf{r}),\begin{cases}\rho'(\mathbf{r})(1-R)^{1/2} & \text{if } R\le 1\\ 0 & \text{if } R>1\end{cases}\right) \quad (11)$$

where we have simplified the equation by just writing R for the functional $R[\rho(\mathbf{r}),\Pi(\mathbf{r})]$, defined in eq 10. To summarize, eq 11 is our postulated on-top density functional as obtained by a "translation" protocol from a GGA; it is not derived from eqs 9 and 10; rather, its form is motivated in part by their form.

3. TEST CASES

MC-PDFT was tested for a variety of cases, including some for which KS-DFT fails or performs poorly. There are four types of tests: (1) multiplet splittings for selected main group atoms (Be, C, N, N^+, O, O^+) and transition metals (Co, Mn, Mo, Ru, and Sc^+); (2) atomic singlet−singlet excitation energy of Be and vertical singlet−singlet excitation energies for N_2, formaldehyde, butadiene, cyclopentadiene, and pyrazine; and (3, 4) equilibrium dissociation energies (D_e) and potential energy curves of the H_2, N_2, F_2, CaO, Cr_2, and NiCl diatomic molecules.

We do not include spin−orbit coupling in any of the calculations. For atomic excitation energies, we removed spin−orbit coupling from the experimental values in the usual way (weighted average of the multiplet). However, for the molecules, we ignore this step since the necessary data are not available for all cases, but this correction should be small for the molecules, because they contain no atom heavier than Ni.

Calculations on singlet−singlet excitation energies were performed at fixed geometries obtained with the M06-L[94] exchange-correlation functional and the 6-311+G(d,p)[95−97] basis set, except for cyclopentadiene for which we used the 6-31+G(2d,p)[95,97−99] basis set.

Calculations of bond energies were performed at consistently optimized geometries. For CaO and NiCl, as for the other molecules, the bond energy is defined as the energy of the neutral atoms in their ground states minus the energy of the molecule at its ground-state optimized geometry. However, note that the separated-atom ground state of CaO is a triplet (Ca ^{1}S plus O ^{3}P); therefore, Table 4 is based on this triplet, whereas Figure 5 shows the singlet potential curve (CaO $^1\Sigma^+$). Similarly the separated-atom limit for NiCl is triplet Ni (^{3}F) + doublet Cl (^{2}P), whereas Figure 6 shows the doublet potential curve (NiCl $^2\Pi$).

4. COMPUTATIONAL DETAILS

In addition to MC-PDFT results, we report results obtained via CASSCF, CASPT2, and KS-DFT for comparison. The MC-PDFT method was implemented in a locally modified version of the *Molcas* program package.[100] All MC-PDFT, CASSCF, and CASPT2 calculations were performed using *Molcas*. All KS-DFT calculations were performed with the Gaussian 09 program.[101]

Basis Sets. We employed basis sets of multiply polarized triple-ζ and quadruple-ζ quality. In the article itself, we report the triple-ζ results, while the quadruple-ζ ones are reported in the Supporting Information (SI). For the various calculations (CASSCF, CASPT2, MC-PDFT, and KS-DFT) on the same system, we use the same basis set.

For the calculations presented in the article itself, we use the following basis sets. For the multiplicity-changing excitation energies of the main-group atoms and diatomic molecules, CaO, and the singlet-to-singlet excitation energies except for N_2 and butadiene, we used the cc-pVTZ[102] basis set. For excitation energies of N_2 and butadiene, we used aug-cc-pVTZ.[103] The Cr_2 calculations employ the cc-pVTZ-DK[104] basis set. For the NiCl and transition-metal atom calculations, we used the ANO-RCC-VTZP[105,106] basis set. For Cr_2, NiCl, and the transition-metal atoms, the second-order Douglas−Kroll−Hess Hamiltonian was used;[90] the other calculations are nonrelativistic.

CASSCF. For each system, the minimal-size active space that gives qualitatively correct results was employed. The active spaces are specified in footnotes to the tables; the same active spaces were used for the figures. In some cases, results for other active spaces are reported in the SI.

CASPT2. For CASPT2, an imaginary shift is introduced to remove problems with intruder states (states giving small denominators in second-order perturbation, and hence having a spuriously large effect on the energy, even when they are weakly coupled to the ground state), and an ionization-potential−electron-affinity (IPEA) shift is introduced as an empirical adjustment to the energies of the active orbitals to improve agreement with the experiment. We employ the standard imaginary shift[107] of 5.44 eV and the *Molcas* default IPEA shift[108] of 6.80 eV. [For Cr_2, one can obtain better CASPT2 results with a molecule-specific IPEA[109] of 12.25 eV, but we do not consider such molecule-specific empirical adjustments in this article.]

KS-DFT. We use collinear spin orbitals, and we consider three exchange-correlation functionals: one of which is a local-spin-density approximation (LSDA), and the other two of which are generalized gradient approximations (GGAs). The LSDA depends only on ρ and m, not on ρ'; it employs the exchange potential of Gáspár[110] (equal to two-thirds of that used by Slater[111] and the same as used later by Kohn and Sham[1]), and correlation potential No. 3 of Vosko et al.[112] This is labeled GVWN3. The GGAs depend on ρ, m, ρ', and m'; the ones we employ are the popular BLYP[112,113] and PBE[114] functionals.

In KS-DFT, with approximate exchange-correlation functionals, the calculated energy is not independent of the M_S value of the Slater determinant (even though it should be). Therefore, one does the calculation with M_S equal to S, where S is the total electronic spin quantum number of the target state. We carried out KS-DFT calculations in two ways,[16] which we call variational (Var) and weighted-average broken symmetry (WABS). Both types of calculations are based on the stable, broken-symmetry solutions of the Kohn−Sham equations in which the only symmetry enforced is the total electron spin component M_S. Thus, when SCF convergence is attained, we do a stability check.[115,116] If the solution is unstable, we break the symmetry and continue optimizing the orbitals until a stable solution is attained. In the Var method, we take this as the energy of the state; this would be the correct procedure if one had the (unknown and probably unknowable) exact Kohn−Sham functional. In the WABS method,[14,15,17−21] if M_S equals one-half the number of singly occupied orbitals (such a state is called a maximal-M_S state), the result is the same as in the Var method. However, if M_S is smaller, we also perform a calculation on the state with maximal M_S and use the weighted average formula of Yamaguchi and co-workers[14,15] to calculate the energy of the pure spin state.

Table 1. Main Group Atomic Excitation Energies (eV)

	Excitation Energy (eV)												
							BLYP		PBE		GVWN3		
transition	AS[a]	CASSCF	CASPT2	tBLYP	tPBE	tGVWN3	Var	WABS	Var	WABS	Var	WABS	Exp
Be $^1S \rightarrow {}^3P$	2, 4	2.9	2.8	2.6	2.6	2.6	2.5	2.5	2.3	2.3	2.4	2.4	2.73[b]
C $^3P \rightarrow {}^1D$	4, 4	1.6	1.3	1.0	1.1	1.0	0.3	0.7	0.4	0.8	0.6	1.3	1.26[c]
N^+ $^3P \rightarrow {}^1D$	4, 4	2.2	1.9	1.5	1.5	1.4	0.6	1.1	0.6	1.2	0.9	1.9	1.89[c]
N $^4S \rightarrow {}^2D$	5, 4	2.8	2.5	1.8	1.9	1.8	0.9	1.4	1.1	1.6	1.5	2.3	2.38[c]
O^+ $^4S \rightarrow {}^2D$	5, 4	3.7	3.4	2.4	2.5	2.5	1.4	2.1	1.5	2.3	2.1	3.2	3.32[d]
O $^3P \rightarrow {}^1D$	6, 4	2.2	2.0	1.2	1.3	1.2	0.7	1.3	0.7	1.4	0.9	1.8	1.96[c]
mean absolute error, MAE[e]		0.3	0.07	0.5	0.5	0.5	1.2	0.8	1.2	0.7	0.9	0.12	

[a]The active space (AS) choices are given for each atom with the notation *n*, *m*, where *n* is the number of active electrons, and *m* is the number of active orbitals. In this table, the active spaces include the valence 2*s* and 2*p* orbitals. [b]Data taken from ref 123. [c]Data taken from ref 124. [d]Data taken from ref 125. [e]Mean unsigned deviation from the experimental value.

Table 2. Transition Metal Atomic Excitation Energies

	Atomic Excitation Energy (eV)												
							BLYP		PBE		GVWN3		
transition	AS[a]	CASSCF	CASPT2	tBLYP	tPBE	tGVWN3	Var	WABS	Var	WABS	Var	WABS	Exp
Sc^+ $^3D \rightarrow {}^1D$	2, 6	0.4	0.3	0.5	0.5	0.4	0.2	0.3	0.2	0.5	0.2	0.5	0.30[b]
Mn $^6S \rightarrow {}^8P$	7, 9	2.2	2.3	2.4	2.2	2.4	2.9	2.9	2.3	2.3	2.6	2.6	2.15[b]
Co $^4F \rightarrow {}^2F$	9, 6	2.3	0.4	1.0	0.9	0.8	0.7	1.0	0.7	1.0	0.3	0.5	0.89[b]
Mo $^7S \rightarrow {}^5S$	6, 6	1.7	1.7	1.8	2.0	1.9	0.9	1.1	1.3	1.6	1.4	1.6	1.34[c]
Ru $^5F \rightarrow {}^3F$	8, 6	1.0	1.0	0.9	1.1	0.9	0.6	0.8	0.7	0.9	0.7	0.9	0.78[d]
mean absolute error, MAE[e]		0.4	0.3	0.2	0.2	0.2	0.3	0.2	0.11	0.2	0.2	0.3	

[a]The active space choices are given for each atom with the notation *n*, *m*, where *n* is the number of active electrons and *m* is the number of active orbitals. For Sc^+ and Co, the active space consists of the 3*d* and 4*s* orbitals. For Mn, the active space includes the 3*d*, 4*s*, and 4*p* orbitals. For Mo and Ru, the active space includes the 4*d* and 5*s* orbitals. [b]Data taken from ref 126. [c]Data taken from ref 127. [d]Data taken from ref 128. [e]Mean unsigned deviation from the experimental value.

The singlet-to-singlet excitation energies considered here all correspond to an excitation that changes the spatial symmetry. We enforce the spatial symmetry in these cases so that we can calculate the KS-DFT excitation energies by the difference of two SCF calculations, without needing to use time-dependent response methods.

MC-PDFT. The CASSCF wave functions generated by the *Molcas* program are computed for a specified total spin and spinprojection, but both the density and the on-top pair density are singlet-spin quantities and are therefore Independent of spin-projection and, hence, no ambiguity about which M_S value to use and no spurious dependence on M_S.[91] To illustrate MC-PDFT, we implement it in this article as follows:

(a) calculate a CASSCF wave function self-consistently;
(b) calculate ρ, Π, and ρ' from the CASSCF wave function;
(c) calculate the on-top density functional using eq 11; and
(d) calculate the energy (post-SCF) by eq 6, which involves an integration over all values of $\mathbf{r}$ of the translated density functionals obtained by eq 11.

The translated on-top density functionals are called tVWN3, tBLYP, and tPBE (the prefix "t" is used to denote "translated").

5. RESULTS

Tables 1 and 2 give multiplicity-changing excitation energies of atoms. Table 3 gives singlet-to-singlet excitation energies, and Table 4 gives equilibrium bond dissociation energies. All mean errors in tables are computed from unrounded data, not from the rounded data in the tables. Figures 1−6 show potential energy curves for diatomic molecules that compare the CASSCF, CASPT2, tPBE, PBE variational, and PBE WABS results. To increase clarity, we left the tBLYP, tGVWN3, BLYP variational, BLYP WABS, GVWN3 variational, and GVWNM3 WABS results out of these figures, but additional figures containing these results are provided in the SI. Figures 7 and 8 show the value of the pair density, total density, and ratio *R* along the bond axis of H_2 and N_2.

6. DISCUSSION

For main-group atomic multiplicity-changing excitation energies, given in Table 1, CASSCF has a mean absolute error (MAE) of 0.3 eV. Variational and WABS KS-DFT calculations with GGAs have much larger errors, with MAEs near 0.7 eV and 1.2 eV, respectively; variational GVWN3 calculations also have a large error (0.9 eV), but WABS GVWN3 does quite well, with an MAE of only 0.12 eV. The MC-PDFT calculations with tBLYP, tPBE, and tGVWN3 all have an MAE of 0.5 eV, much better than the average (0.8 eV) of the six KS-DFT results. The SI shows that the transformed functional performance is approximately independent of basis set size and almost independent of active space size, although the MAE can be reduced to 0.3 eV with other active space choices; however, in the rest of the main article, we concentrate on what is achieved with the smallest reasonable complete active space choices and triple-ζ basis sets, rather than search for the lowest possible errors. We conclude that, on average, the translated functionals perform better (0.5 eV) than their KS-DFT counterparts (0.8 eV). The MC-PDFT calculations perform slightly worse than CASSCF and CASPT2.

Table 2 shows that, for transition-metal atoms, the excitation energies obtained by the MC-PDFT calculations with the translated functionals are better (MAE: 0.2 eV) than CASSCF

dx.doi.org/10.1021/ct500483t | J. Chem. Theory Comput. 2014, 10, 3669−3680

Table 3. Singlet-to-Singlet Atomic and Vertical Electronic Excitation Energies (eV)

system	Excitation Energy (eV)									
	AS[a]	CASSCF	CASPT2	tBLYP	tPBE	tGVWN3	BLYP	PBE	GVWN3	Exp
Be $^1S \rightarrow {}^1P$ ($s \rightarrow p$)	2, 4	6.2	5.7	4.2	4.4	4.3	5.0	5.0	5.0	5.28[b]
N_2 $^1\Sigma_g^+ \rightarrow {}^1\Pi_g$ ($\sigma_g \rightarrow \pi_g$)	6, 6	11.9	9.4	8.6	8.6	8.6	9.1	9.1	9.1	9.31[c]
N_2 $^1\Sigma_g^+ \rightarrow {}^1\Sigma_u^-$ ($\pi_u \rightarrow \pi_g$)	6, 6	10.9	9.8	9.5	9.6	9.6	9.6	9.7	9.7	9.92[c]
s-trans-1,3-butadiene ^1A_g to ^1B_u ($\pi \rightarrow \pi^*$)	4, 4	7.6	6.8	5.6	5.7	5.9	5.3	5.5	5.5	5.92[d]
pyrazine ^1A_g to $^1B_{3u}$ ($n \rightarrow \pi^*$)	10, 10	5.3	4.1	3.9	3.9	3.8	3.6	3.6	3.5	4.20[e]
cyclopentadiene $^1A_1$ to $^1B_2$ ($\pi \rightarrow \pi^*$)	4, 4	7.3	5.5	4.1	4.1	4.1	4.9	5.0	5.0	5.26[f,g]
formaldehyde $^1A_1$ to $^1A_2$ ($I \rightarrow \pi^*$)	8, 6	4.4	4.0	4.0	4.0	4.0	4.0	3.9	3.8	4.00[h]
mean absolute error, MAE[i]		1.4	0.3	0.6	0.5	0.5	0.3	0.3	0.3	

[a]For Be and N_2, the active space (AS) in each case is the full valence active space. For *s-trans*-1,3-butadiene, cyclopentadiene, and pyrazine, the AS includes the π electrons, π bonding and antibonding orbitals, and additional nitrogen lone pairs/orbitals for pyrazine. For formaldehyde, the AS includes all the electrons, lone pair orbitals, and bonding and antibonding orbitals of the carbonyl. [b]Data taken from ref 129. [c]Data taken from ref 130. [d]Data taken from ref 131. [e]Data taken from ref 132. [f]Data taken from ref 133. [g]Data taken from ref 134. [h]Data taken from ref 135. For N_2, an equilibrium geometry of 1.098 Å was used.[4] All other geometries were optimized according to specifications in Table S5 in the SI with M06-L.[3] [i]Mean unsigned deviation from the experimental value.

(0.4 eV) or CASPT2 (0.3 eV) and comparable to KS-DFT (mean MAE of 0.2 eV when averaged over either the three variational sets of the three WABS sets of results). Averaging over the main group and transition-metal results, one finds that MC-PDFT is already (that is, even with these first attempts at on-top functionals) better, on average, than CASSCF or KS-DFT, but not systematically better than the much more expensive and less favorably scaling CASPT2.

Inspection of Table 3 shows that MC-PDFT calculations with the translated functionals succeed in performing much better (average MAE = 0.5 eV) than CASSCF (MAE = 1.4 eV) in predicting vertical excitation energies. MC-PDFT performs better than KS-DFT for butadiene, pyrazine, and formaldehyde, but not for the other four cases. MC-PDFT is more accurate than CASPT2 for butadiene and has the same accuracy for formaldehyde, but on average is less accurate than the more expensive method. The relatively good results for butadiene are especially interesting, since this molecule is a case in which both the ground and excited states have substantial double excitation character.[117]

Figures 1−6 show that MC-PDFT fulfills one of its major goals, namely, the calculation of reasonable potential energy curves for bond breaking. The results for Cr_2 in Figure 5 are particularly striking, because the CASSCF curve does not even have a minimum, and the CASPT2 curve has a minimum energy at a qualitatively wrong geometry. The tPBE curve has a minimum at a reasonable geometry. By changing the IPEA shift in CASPT2 the curve has much better agreement with the experimental result,[109] but here we prefer to compare with only the standard CASPT2 method.

For bond energies of the diatomic molecules considered in Table 4, the translated GGAs, with MAE values of 0.3 and 0.4 eV, perform better than KS-DFT for the BLYP and PBE functionals (MAE = 0.5−0.6 eV), and the translated GVWN3 performs better (MAE = 0.9 eV) than GVWN3 (MAE = 1.4−1.5 eV). MC-PDFT also improves upon CASSCF (MAE = 0.8 eV). The results for bond energies are especially encouraging, because of the diversity of cases involved: a closed-shell single bond with no static correlation error (H_2), a closed-shell single bond with large static correlation error if treated by Hartree−Fock (F_2), a triple bond (N_2), singlet and doublet polar molecules involving metal atoms (CaO and NiCl), and the notoriously difficult Cr_2 molecule.

One of the main reasons why we developed MC-PDFT is to avoid the ambiguity and resulting inaccuracy of using broken-symmetry solutions for inherently multiconfigurations systems. Molecules with partially broken bonds (that is, highly stretched bonds) are the most commonly encountered class of such multireference systems. In order to study how well the present method performs for such cases, the figures show magnified views of the intermediate-bond-distance regions of the potential as panel (b) in five of the first six figures. The results are generally encouraging. See especially Figures 2b, 3b, 4b, and 6b, where the MC-PDFT results with tPBE functionals follow the CASPT2 curves better than either the Var KS-DFT results or the WABS KS-DFT results.

The good results obtained for N_2 and Cr_2 dissociation are especially noteworthy, because these are both difficult cases. They both involve dissociation to highly open-shell atoms with three or more unpaired electrons. While KS-DFT can properly describe N_2 at equilibrium, because it is a closed-shell singlet, KS-DFT can only obtain reasonable results for Cr_2 at equilibrium by treating it as two antiferromagnetically coupled high-spin atoms in a broken-symmetry solution. The ability of the new theory to treat these most-difficult cases shows that the on-top pair density is successful, not just for breaking a single bond in systems such as H_2 and F_2, but also in providing a qualitatively correct description for more-complicated bond-breaking processes requiring the spin recoupling of more than one electron pair.

For both H_2 and N_2, the success of the on-top pair density in describing molecular dissociations is shown in Figures 7 and 8. In the limit of a closed-shell singlet at equilibrium, $R(z) = 1$. Figures 7 and 8 show the densities, on-top pair densities, and the ratio R of eq 11, each as functions of location z along the internuclear axis for dissociating H_2 and N_2. In the limit of infinite separation for H_2 in Figure 7b, $R(z) = 0$, because the value of the on-top pair density is zero (corresponding to one electron on each center). In Figure 8b, we show how the on-top pair density behaves for an intermediate distance along the potential energy curve.

Just as CASPT2 and other WFT methods for including dynamical correlation energy are employed as post-SCF steps, the present version of MC-PDFT is employed as a post-SCF procedure. If the density functional were to be dependent only on the one-particle density matrix, the equations for the self-consistent CASSCF wave function (in which the wave function is optimized to minimize the MC-PDFT energy rather than the expectation value of the Hamiltonian) would be an indetermi-

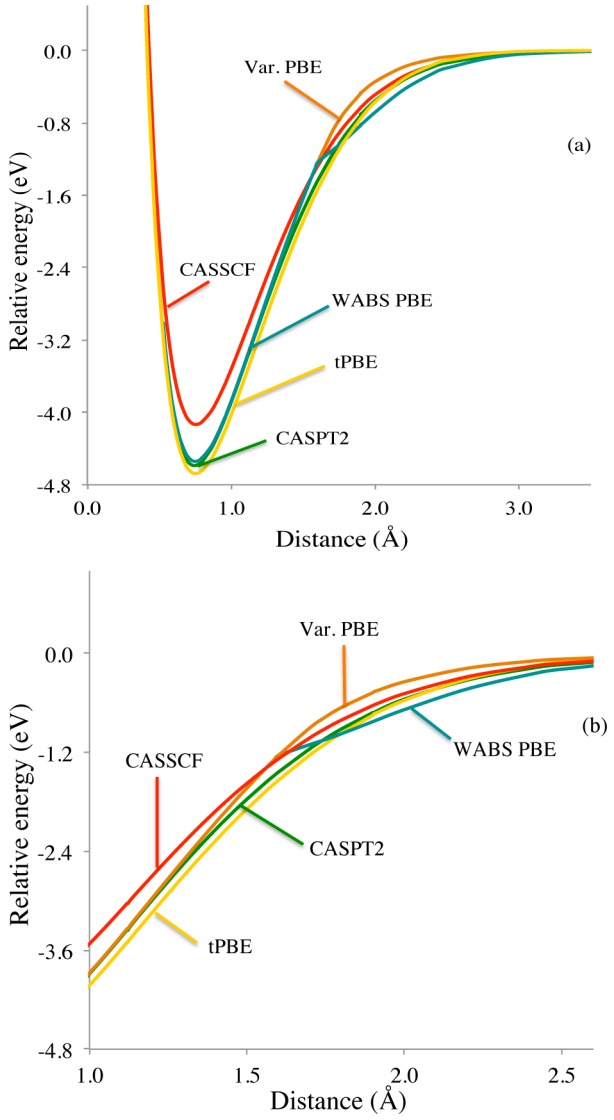

Figure 1. Potential energy curves for H_2: (a) at equilibrium, the Var and WABS curves for each functional are the same, but they are different at intermediate distances (the CASPT2 minimum is just below the WABS PBE minimum, and the entire range of distances is shown); (b) magnification of the region of 1−3 Å (the WABS curves are lower in energy than the Var counterparts at intermediate distances).

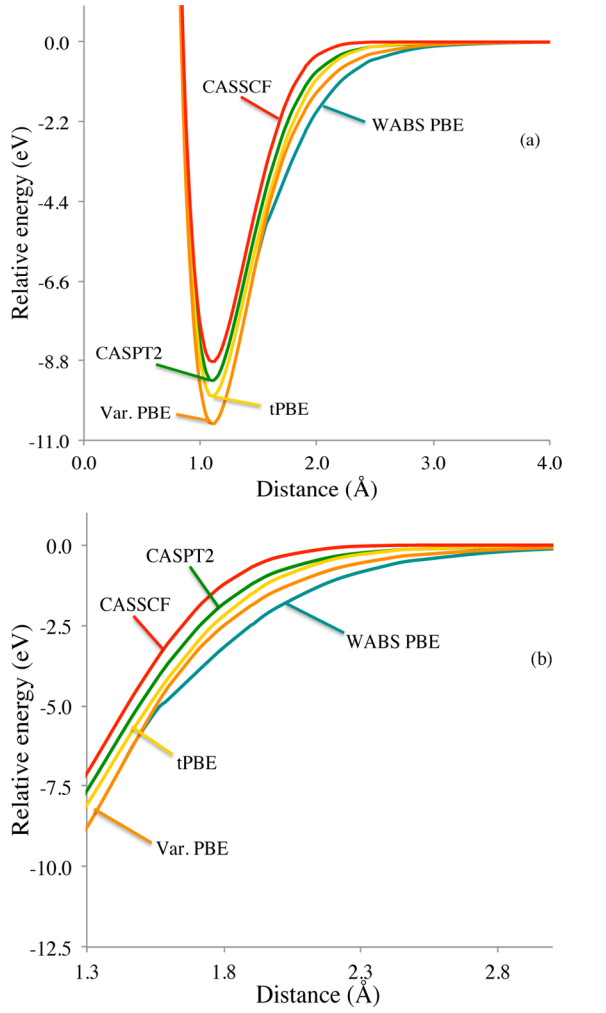

Figure 2. Potential energy curves for N_2: (a) at equilibrium, the Var and WABS curves for each functional are the same, but they are different at intermediate distances (the entire range of distances is shown); (b) magnification of the region of 1.3−2.8 Å.

nate system of equations, because a one-electron operator does not couple configurations differing by two orbitals, and there would be no unique solution. However, our on-top density functional is also dependent on part of the two-particle density matrix; nevertheless, we include the energy contribution of the on-top density functional as a post-SCF step.

Another topic for future work would be to develop foundational theorems, if possible, about the existence and uniqueness of an exact on-top density functional for use with MC-PDFT. However, we note that the immediate goal of the present new type of DFT is not to extend Kohn−Sham theory to classes of systems where the density does not belong to the representability class for which Kohn−Sham theory is applicable and exact,[118−122] but rather to develop a practical framework for obtaining less-ambiguous and/or more-accurate densities and energies for systems where Kohn−Sham theory with approximate exchange-correlation functionals does not perform well.

7. CONCLUDING REMARKS

We have presented a theory called Multiconfiguration Pair-Density Functional Theory (MC-PDFT). The kinetic and Coulomb contributions to the total electronic energy are computed from an optimized MCSCF wave function, and the exchange and correlation contributions are computed from a functional of the total density and the on-top pair density; this functional is called the "on-top density functional". Just as for exchange-correlation functionals in Kohn−Sham density functional theory (DFT), the on-top density functional can also be a function of functionals of the density. For example, it could be dependent on the density gradient or the orbital-dependent kinetic energy density. For a first set of approximate on-top density functionals, we use functionals of the density, the density gradient, and the on-top density that we obtain by translating Kohn−Sham exchange-correlation functionals according to a simple prescription. Also, we would like to eventually include the dependence on the pair-density gradient and the kinetic energy density.

The presented theory has been used in combination with the tBLYP, tPBE, and tGVWN3 on-top density functionals generated from the BLYP, PBE, and GVWN3 exchange-correlation functionals. Results with the translated functionals

dx.doi.org/10.1021/ct500483t | J. Chem. Theory Comput. 2014, 10, 3669−3680

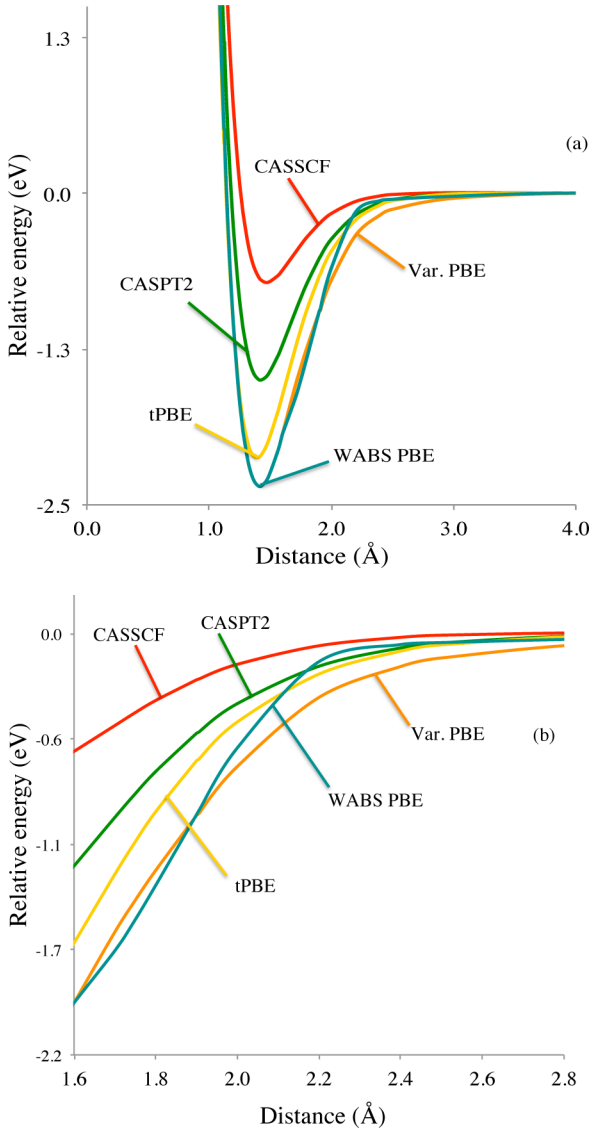

Figure 3. Potential energy curves for F_2: (a) at equilibrium, the Var and WABS curves for each functional are the same, but they are different at intermediate distances (the entire range of distances is shown); (b) magnification of the region of 1.6−2.8 Å.

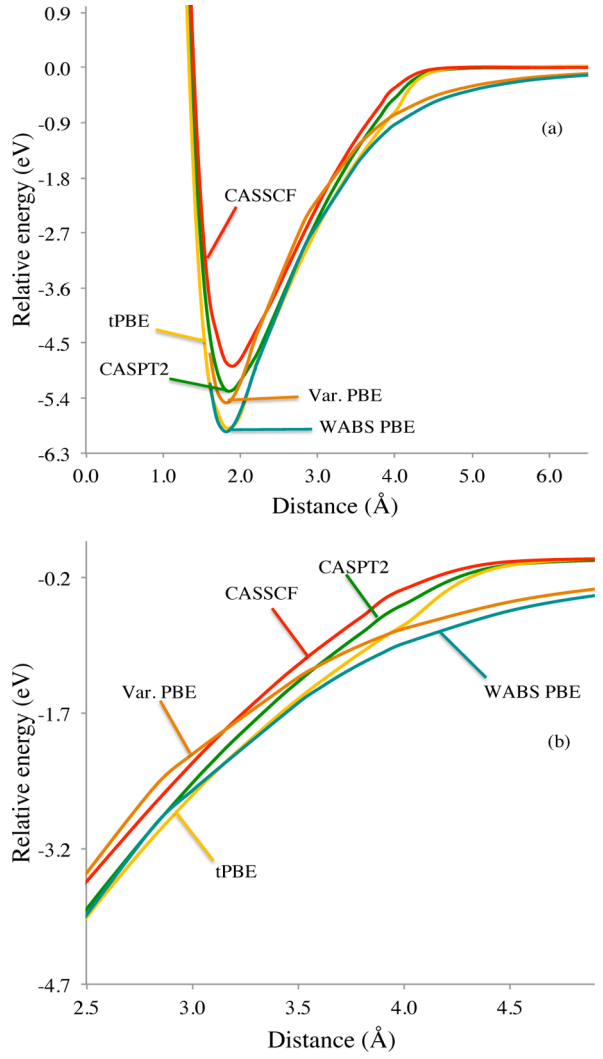

Figure 4. Potential energy curves for the $^1\Sigma^+$ state of CaO: (a) the CASPT2 and tPBE curves are very close at equilibrium and, therefore, are hard to distinguish in the figure (the entire range of distances is shown); (b) magnification of the region of 2.5−5.5 Å.

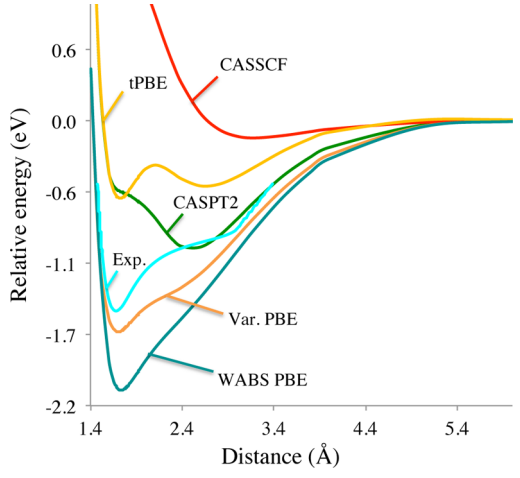

Figure 5. Potential energy curves for Cr_2. The experimental curve (Casey and Leopold, ref 93) is shown for experimentally measurable distances and is shifted to a common asymptote by the experimentally determined dissociation energy.

have been generated for a variety of systems and compared with the corresponding results at the CASSCF, CASPT2, and Kohn−Sham DFT levels. This method is promising. To provide a better overview of the results, Table 5 provides a survey of the average mean absolute error (MAE) values given in Tables 1−4. We see that the first results with the new theory, using simply translated GGA functionals, reduce the error in CASSCF by an average of almost a factor of 2 and are ∼20% more accurate than Kohn−Sham theory, based on the same GGAs. This theory even produces results whose quality is similar to that of the much more expensive CASPT2 method for two of the four databases. The basis set dependence is smaller than for CASPT2, and the troublesome problem of intruder states does not arise. In the future, we plan to develop new functionals of the total density and on-top pair density, which will be optimized for use with multiconfigurational wave functions. We will also employ RASSCF, GASSCF, and SplitGAS wave functions to be able to deal with larger active spaces and CI problems than those that are currently affordable with CASSCF.

dx.doi.org/10.1021/ct500483t | J. Chem. Theory Comput. 2014, 10, 3669−3680

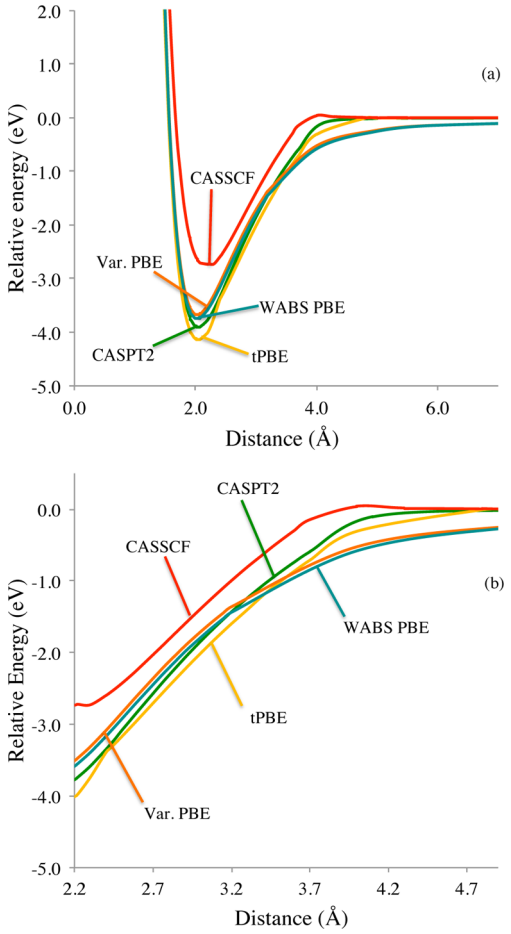

Figure 6. Potential energy curves for the $^2\Pi$ state of NiCl: (a) at equilibrium, the electronic structure is ionic, with Ni^+ having a $3d^9$ configuration, and at dissociation, Ni is in its $3d^84s^2$ ground state (the entire range of distances is shown); (b) magnification of the region of 2.5−5.5 Å.

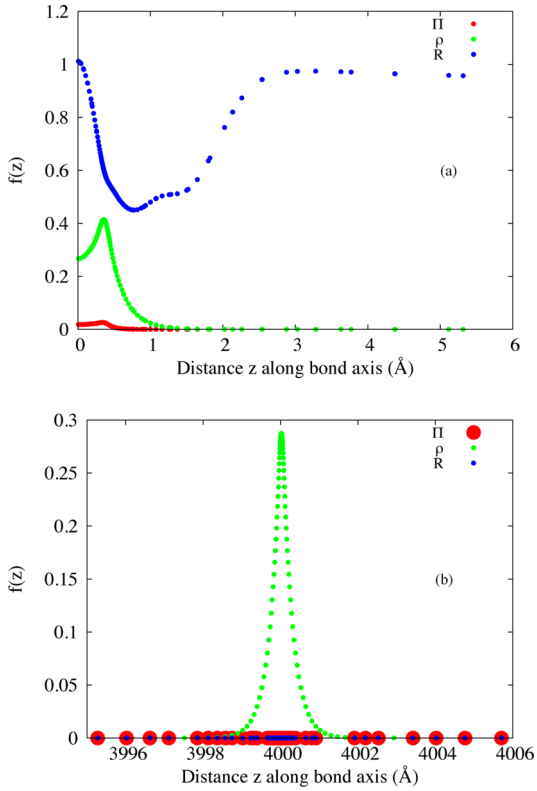

Figure 7. Plots of the pair density, total density, and the ratio for H_2 (quantities denoted as $f(z)$) along the bond axis (in the plot, 0 Å is the middle of the bond between the atoms): (a) at equilibrium (only one atom of the dimer is represented in the plot, centered at ∼0.35 Å) and (b) at dissociation.

The advantages of the new theory may be summarized as follows:

(i) It can correctly describe inherently multiconfigurational systems, including ground states and singly and doubly excited states or any states that are qualitatively well-described by the chosen MCSCF wave function.

Table 4. Dissociation Energies of Diatomic Molecules

	Dissociation Energy (eV)												
							BLYP		PBE		GVWN3		
dimer	AS[a]	CASSCF	CASPT2	tBLYP	tPBE	tGVWN3	Var	WABS	Var	WABS	Var	WABS	Exp
H_2	2, 2	4.1	4.6	4.9	4.7	5.0	4.8	4.8[b]	4.5	4.5[b]	4.9	4.9[b]	4.75[c]
N_2	6, 6	8.8	9.4	9.4	9.8	11.1	10.4	10.4[b]	10.6	10.6[b]	11.9	11.9[b]	9.74[d]
F_2	2, 2	0.9	1.5	1.9	2.1	2.8	2.2	2.2[b]	2.4	2.4[b]	3.5	3.5[b]	1.66[e]
Cr_2	12, 12	0[f]	1.0	0.5	0.6	2.3	2.1	2.5	1.6	2.1	3.5	3.7	1.47[g]
CaO	8, 8	3.9	3.5	4.0	4.2	5.2	4.7	4.7[h]	5.0	5.0[h]	6.1	6.1[h]	4.22[i]
NiCl	11, 12	2.7	3.9	3.5	4.1	4.8	3.4	3.7	3.7	3.7	4.5	4.6	3.97[j,k]
mean absolute error, MAE[l]		0.8	0.3	0.4	0.3	0.9	0.5	0.5	0.5	0.6	1.4	1.5	

[a]The active space (AS) choice for H_2 and N_2 includes the bonding electrons and bonding/antibonding orbitals. For F_2, the active space includes one 2*p* electron and orbital on each atom contributing to the ^{2}P configuration of the neutral atom. For Cr_2, the active space includes the *d* and 4*s* electrons and orbitals on each atom. The AS for CaO includes the 4*s* electrons on Ca and the 2*s* and 2*p* electrons on O. In addition to these orbitals, there is a correlating 4*p* shell on Ca. For NiCl, the active space includes the 4*s* and 3*d* electrons on Ni and one 2*p* electron and orbital on Cl that contributes to the ^{2}P configuration of the neutral atom. [b]The WABS dissociation energy is the same as variational one, because this case has no spin contamination at the equilibrium geometry. [c]Data taken from ref 136. [d]Data taken from ref 137. [e]Data taken from ref 138. [f]The potential curve has no minimum in this case; see Figure 5. [g]Data taken from ref 139. [h]The WABS dissociation energy is the same as the variational dissociation energy in this case, because there is negligible spin contamination in the ground-state triplet asymptote that is used to compute the dissociation energy from the singlet equilibrium ground state, whereas the Var and WABS curves in Figure 4 differ, because they are relative to the singlet asymptote. [i]Data taken from ref 140. [j]Data taken from ref 141. [k]Data taken from ref 142. [l]Mean unsigned deviation from the experimental value.

dx.doi.org/10.1021/ct500483t | J. Chem. Theory Comput. 2014, 10, 3669−3680

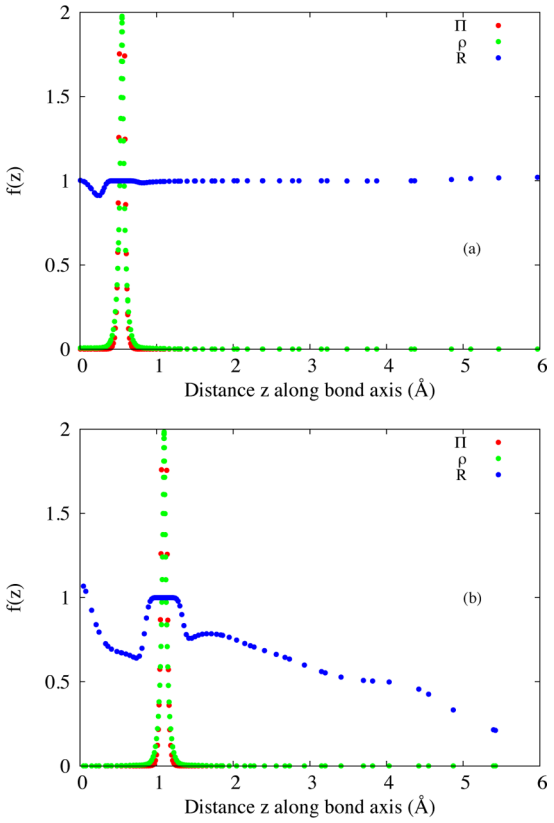

Figure 8. Plot of the pair density, total density, and the ratio for N_2 (quantities denoted as $f(z)$) along the bond axis (in the plot, 0 Å is the middle of the bond between the atoms; the pair density and total density have been scaled in this figure by factors of 1000 and 100, respectively): (a) at equilibrium (only one atom of the dimer is represented in the plot, centered at ∼0.55 Å) and (b) at 2*Re*.

Table 5. Averaged Mean Absolute Error (MAE) Values

	Mean Absolute Error, MAE (eV)			
quantity	CASSCF	CASPT2	tGGA[a]	GGA[b]
main group atomic excitation energies	0.29	0.07	0.48	1.01
transition-metal atomic excitation energies	0.41	0.26	0.23	0.21
singlet-to-singlet molecular excitation energies	1.39	0.26	0.55	0.33
bond dissociation energies	0.89	0.32	0.33	0.51
average	0.75	0.23	0.40	0.52

[a]Averaged over tBLYP and tPBE. [b]Averaged over BLYP Var, BLYP WABS, PBE Var, and PBE WABS (see Figure 1a).

(ii) Because all states have the correct spin and spatial symmetry, there are no ambiguities about which state is being approximated.

(iii) There is no spurious dependence on the spin projection quantum number.

(iv) Its computational cost scales with system size in the same way as CASSCF (the cost depends on the choice of active space), but produces results similar to (and sometimes better than) CASPT2 quality.

(v) Unlike prior attempts to combine CASSCF and DFT, which combine a portion of the energy calculated by wave function methods with another portion calculated from a density functional, the present method avoids any possibility of double-counting of the electron correlation energy.

(vi) The new method has a moderate dependence on the active space choice, or at least a smaller dependence than CASPT2. This is a promising feature, because, ideally, one would like to work with a small active space.

■ ASSOCIATED CONTENT

Ⓢ Supporting Information

Geometries of all optimized structures (values given in Å), additional tables of excitation energies (values given in eV) calculated with other active spaces and basis sets, and additional figures of potential curves. This material is available free of charge via the Internet at http://pubs.acs.org/.

■ AUTHOR INFORMATION

Corresponding Authors

*E-mail: truhlar@umn.edu (D. G. Truhlar).

*E-mail: gagliardi@umn.edu (L. Gagliardi).

Author Contributions

§These four authors (GLM, RKC, SL, DM) contributed equally.

Notes

The authors declare no competing financial interest.

■ ACKNOWLEDGMENTS

We acknowledge the authors of ref 42 for making the routines for computing CASSCF densities and on-top pair densities available for experimentation. This material is based upon work supported by the National Science Foundation (NSF) (under Grant No. CHE−1212575) (R.C., and L.G.). This work was also supported by the U.S. Air Force (under Grant No. FA9550-11-1-0078) (S.L., D.T.). Support for D.M., and G.L.M. was provided through Scientific Discovery through Advanced Computing (SciDAC) program funded by U.S. Department of Energy, Office of Science, Basic Energy Sciences and Advanced Scientific Computing Research under Award No. DE-SC0008666.

■ REFERENCES

(1) Kohn, W.; Sham, L. *Phys. Rev.* **1965**, *140*, A1133−A1138.

(2) Engel, E.; Dreizler, R. M. *Density Functional Theory*; Springer−Verlag: Berlin, 2011.

(3) Jacob, C. R.; Reiher, M. *Int. J. Quantum Chem.* **2012**, *112*, 3661−3684.

(4) Lowdin, P. O. *Phys. Rev.* **1955**, *97*, 1474−1489.

(5) Kohn, W. *Rev. Mod. Phys.* **1999**, *71*, 1253−1266.

(6) Mok, D. K. W.; Neumann, R.; Handy, N. C. *J. Phys. Chem.* **1996**, *100*, 6225−6230.

(7) Handy, N. C.; Cohen, A. J. *Mol. Phys.* **2001**, *99*, 403−412.

(8) Hollett, J. W.; Gill, P. M. W. *J. Chem. Phys.* **2011**, *134*, 1141111.

(9) Schuch, N.; Verstraete, F. *Nat. Phys.* **2009**, *5*, 732−735.

(10) Pederson, M. R.; Ruzsinszky, A.; Perdew, J. P. *J. Chem. Phys.* **2014**, *140*, 121103.

(11) Schultz, N. E.; Zhao, Y.; Truhlar, D. G. *J. Phys. Chem. A* **2005**, *109*, 11127−11143.

(12) Harvey, J. N. *Annu. Rep. Prog. Chem. C* **2006**, *102* (1), 203−226.

(13) Cohen, A. J.; Mori-Sanchez, P.; Yang, W. T. *Science* **2008**, *321*, 792−794.

(14) Yamaguchi, K.; Tsunekawa, T.; Toyoda, Y.; Fueno, T. *Chem. Phys. Lett.* **1988**, *143*, 371−376.

(15) Yamaguchi, K.; Jensen, F.; Dorigo, A.; Houk, K. N. *Chem. Phys. Lett.* **1988**, *149*, 537−542.

(16) Luo, S. J.; Averkiev, B.; Yang, K. R.; Xu, X. F.; Truhlar, D. G. *J. Chem. Theory Comput.* **2014**, *10*, 102−121.

(17) Noodleman, L. *J. Chem. Phys.* **1981**, *74*, 5737−5743.

(18) Nishino, M.; Yamanaka, S.; Yoshioka, Y.; Yamaguchi, K. *J. Phys. Chem. A* **1997**, *101*, 705−712.
(19) Lovell, T.; Liu, T. Q.; Case, D. A.; Noodleman, L. *J. Am. Chem. Soc.* **2003**, *125*, 8377−8383.
(20) Noodleman, L.; Han, W. G. *J. Biol. Inorg. Chem.* **2006**, *11*, 674−694.
(21) Cramer, C. J.; Truhlar, D. G. *Phys. Chem. Chem. Phys.* **2009**, *11*, 10757−10816.
(22) Roos, B. O.; Taylor, P. R.; Siegbahn, P. E. M. *Chem. Phys.* **1980**, *48*, 157−173.
(23) Andersson, K.; Malmqvist, P.-Å.; Roos, B. O. *J. Chem. Phys.* **1992**, *96*, 1218−1226.
(24) Siegbahn, P. E. M.; Almlof, J.; Heiberg, A.; Roos, B. O. *J. Chem. Phys.* **1981**, *74*, 2384−2396.
(25) Malmqvist, P. Å.; Pierloot, K.; Shahi, A. R. M.; Cramer, C. J.; Gagliardi, L. *J. Chem. Phys.* **2008**, *128*, 204109.
(26) Li Manni, G.; Aquilante, F.; Gagliardi, L. *J. Chem. Phys.* **2011**, *134*, 034114.
(27) Ma, D.; Li Manni, G.; Gagliardi, L. *J. Chem. Phys.* **2011**, *135*, 044128.
(28) Li Manni, G.; Ma, D.; Aquiliante, F.; Olsen, J.; Gagliardi, L. *J. Chem. Theory Comp.* **2013**, *9*, 3375−3384.
(29) Ivanic, J. *J. Chem. Phys.* **2003**, *119*, 9364−9376.
(30) Savin, A. Correlation contributions from density functionals. In *Density Functional Methods in Chemistry*; Labanowski, J. K., Andzelm, J. W., Eds.; Springer: Berlin, 1991; pp 213−230.
(31) Miehlich, B.; Stoll, H.; Savin, A. *Mol. Phys.* **1997**, *91*, 527−536.
(32) Grafenstein, J.; Kraka, E.; Cremer, D. *Chem. Phys. Lett.* **1998**, *288*, 593−602.
(33) Malcolm, N. O. J.; McDouall, J. J. W. *Chem. Phys. Lett.* **1998**, *282*, 121−127.
(34) Wu, W.; Shaik, S. *Chem. Phys. Lett.* **1999**, *301*, 37−42.
(35) Grafenstein, J.; Cremer, D. *Chem. Phys. Lett.* **2000**, *316*, 569−577.
(36) He, Y.; Grafenstein, J.; Kraka, E.; Cremer, D. *Mol. Phys.* **2000**, *98*, 1639−1658.
(37) Takeda, R.; Yamanaka, S.; Yamaguchi, K. *Chem. Phys. Lett.* **2002**, *366*, 321−328.
(38) Pollet, R.; Savin, A.; Leininger, T.; Stoll, H. *J. Chem. Phys.* **2002**, *116*, 1250−1258.
(39) Stoll, H. *Chem. Phys. Lett.* **2003**, *376*, 141−147.
(40) McDouall, J. J. W. *Mol. Phys.* **2003**, *101*, 361−371.
(41) Gusarov, S.; Malmqvist, P. A.; Lindh, R.; Roos, B. O. *Theor. Chem. Acc.* **2004**, *112*, 84−94.
(42) Gusarov, S.; Malmqvist, P. A.; Lindh, R. *Mol. Phys.* **2004**, *102*, 2207−2216.
(43) Grafenstein, J.; Cremer, D. *Mol. Phys.* **2005**, *103*, 279−308.
(44) Ukai, T.; Nakata, K.; Yamanaka, S.; Kubo, T.; Morita, Y.; Takada, T.; Yamaguchi, K. *Polyhedron* **2007**, *26*, 2313−2319.
(45) Kurzweil, Y.; Lawler, K. V.; Head-Gordon, M. *Mol. Phys.* **2009**, *107*, 2103−2110.
(46) Sharkas, K.; Savin, A.; Jensen, H. J. A.; Toulouse, J. *J. Chem. Phys.* **2012**, *137*, 044104.
(47) Cagg, B. A.; Rassolov, V. A. *Chem. Phys. Lett.* **2012**, *543*, 205−207.
(48) Goll, E.; Werner, H. J.; Stoll, H.; Leininger, T.; Gori-Giorgi, P.; Savin, A. *Chem. Phys.* **2006**, *329*, 276−282.
(49) Goll, E.; Werner, H. J.; Stoll, H. *Chem. Phys.* **2008**, *346*, 257−265.
(50) Stoyanova, A.; Teale, A. M.; Toulouse, J.; Helgaker, T.; Fromager, E. *J. Chem. Phys.* **2013**, *139*, 134113.
(51) Grimme, S.; Waletzke, M. *J. Chem. Phys.* **1999**, *111*, 5645−5655.
(52) Filatov, M.; Shaik, S. *J. Phys. Chem. A* **2000**, *104*, 6628−6636.
(53) Khait, Y. G.; Hoffmann, M. R. *J. Chem. Phys.* **2004**, *120*, 5005−5016.
(54) Yamanaka, S.; Nakata, K.; Ukai, T.; Takada, T.; Yamaguchi, K. *Int. J. Quantum Chem.* **2006**, *106*, 3312−3324.
(55) Fromager, E.; Toulouse, J.; Jensen, H. J. A. *J. Chem. Phys.* **2007**, *126*.
(56) Perez-Jimenez, A. J.; Perez-Jorda, J. M. *Phys. Rev. A* **2007**, *75*.
(57) Perez-Jimenez, A. J.; Perez-Jorda, J. M.; Moreira, I. D. R.; Illas, F. *J. Comput. Chem.* **2007**, *28*, 2559−2568.
(58) Perez-Jimenez, A. J.; Perez-Jorda, J. M.; Sancho-Garcia, J. C. *J. Chem. Phys.* **2007**, *127*, 104102.
(59) Ukai, T.; Nakata, K.; Yamanaka, S.; Takada, T.; Yamaguchi, K. *Mol. Phys.* **2007**, *105*, 2667−2679.
(60) Nishihara, S.; Yamanaka, S.; Ukai, T.; Nakata, K.; Kusakabe, K.; Yonezawa, Y.; Nakamura, H.; Takada, T.; Yamaguchi, K. *Int. J. Quantum Chem.* **2008**, *108*, 2966−2977.
(61) Weimer, M.; Della Sala, F.; Gorling, A. *J. Chem. Phys.* **2008**, *128*.
(62) Fromager, E.; Cimiraglia, R.; Jensen, H. J. A. *Phys. Rev. A* **2010**, *81*.
(63) Ying, F. M.; Su, P. F.; Chen, Z. H.; Shaik, S.; Wu, W. *J. Chem. Theory Comput.* **2012**, *8*, 1608−1615.
(64) Zhao, Y.; Lynch, B. J.; Truhlar, D. G. *J. Phys. Chem. A* **2004**, *108*, 4786−4791.
(65) Zhao, Y.; Lynch, B. J.; Truhlar, D. G. *Phys. Chem. Chem. Phys.* **2005**, *7*, 43−52.
(66) Tarnopolsky, A.; Karton, A.; Sertchook, R.; Vuzman, D.; Martin, J. M. L. *J. Phys. Chem. A* **2008**, *112*, 3−8.
(67) Zhang, I. Y.; Luo, Y.; Xu, X. *J. Chem. Phys.* **2010**, *132*, 194105.
(68) Sharkas, K.; Toulouse, J.; Savin, A. *J. Chem. Phys.* **2011**, *134*.
(69) Goerigk, L.; Grimme, S. *J. Chem. Theory Comput.* **2011**, *7*, 291−309.
(70) Zhang, I. Y.; Xu, X.; Jung, Y.; Goddard, W. A. *Proc. Natl. Acad. Sci. U. S. A.* **2011**, *108*, 19896−19900.
(71) Zhang, I. Y.; Xu, X. *Int. Rev. Phys. Chem.* **2011**, *30*, 115−160.
(72) Zhang, I. Y.; Su, N. Q.; Bremond, E. A. G.; Adamo, C.; Xu, X. *J. Chem. Phys.* **2012**, *136*, 174103.
(73) Souvi, M. O.; Sharkas, K.; Toulouse, J. *J. Chem. Phys.* **2014**, *140*, 084107.
(74) Perdew, J. P.; Savin, A.; Burke, K. *Phys. Rev. A* **1995**, *51*, 4531−4541.
(75) Lowdin, P. O. *Rev. Mod. Phys.* **1981**, *35*, 496−501.
(76) Becke, A. D.; Savin, A.; Stoll, H. *Theor. Chim. Acta* **1995**, *91*, 147−156.
(77) Moscardo, F.; Sanfabian, E. *Phys. Rev. A* **1991**, *44*, 1549−1553.
(78) Staroverov, V. N.; Davidson, E. R. *Int. J. Quantum Chem.* **2000**, *77*, 651−660.
(79) Heyd, J.; Scuseria, G. E.; Ernzerhof, M. *J. Chem. Phys.* **2003**, *118*, 8207−8215.
(80) Henderson, T. M.; Izmaylov, A. F.; Scuseria, G. E.; Savin, A. *J. Chem. Theory Comput.* **2008**, *4*, 1254−1262.
(81) Chai, J. D.; Head-Gordon, M. *J. Chem. Phys.* **2008**, *128*, 084106.
(82) Chai, J. D.; Head-Gordon, M. *Phys. Chem. Chem. Phys.* **2008**, *10*, 6615−6620.
(83) Peverati, R.; Truhlar, D. G. *J. Phys. Chem. Lett.* **2011**, *2*, 2810−2817.
(84) Peverati, R.; Truhlar, D. G. *Phys. Chem. Chem. Phys.* **2012**, *14*, 16187−16191.
(85) Peverati, R.; Truhlar, D. G. *J. Phys. Chem. Lett.* **2012**, *3*, 117−124.
(86) Tsai, C. W.; Su, Y. C.; Li, G. D.; Chai, J. D. *Phys. Chem. Chem. Phys.* **2013**, *15*, 8352−8361.
(87) Garza, A. J.; Jimenez-Hoyos, C. A.; Scuseria, G. E. *J. Chem. Phys.* **2013**, *138*, 134102.
(88) Garza, A. J.; Jimenez-Hoyos, C. A.; Scuseria, G. E. *J. Chem. Phys.* **2014**, *140*, 244102.
(89) Douglas, N.; Kroll, N. M. *Ann. Phys.* **1974**, *82*, 89−155.
(90) Hess, B. A. *Phys. Rev. A* **1986**, *33*, 3742−3748.
(91) Roos, B. O.; Malmqvist, P. A. *Phys. Chem. Chem. Phys.* **2004**, *6*, 2919−2927.
(92) Perdew, J. P.; Ernzerhof, M.; Burke, K.; Savin, A. *Int. J. Quantum Chem.* **1997**, *61*, 197−205.
(93) Tsuchimochi, T.; Scuseria, G. E.; Savin, A. *J. Chem. Phys.* **2010**, *132*, 024111.
(94) Zhao, Y.; Truhlar, D. G. *J. Chem. Phys.* **2006**, *125*, 194101.
(95) Hariharan, P. C.; Pople, J. A. *Theor. Chim. Acta* **1973**, *28*, 213−222.
(96) Krishnan, R.; Binkley, J. S.; Seeger, R.; Pople, J. A. *J. Chem. Phys.* **1980**, *72*, 650−654.
(97) Clark, T.; Chandrasekhar, J.; Spitznagel, G. W.; Schleyer, P. v. R. *J. Comput. Chem.* **1983**, *4*, 294−301.

(98) Hehre, W. J.; Ditchfield, R.; Pople, J. A. *J. Chem. Phys.* **1972**, *56*, 2257−2261.
(99) Frisch, M. J.; Pople, J. A.; Binkley, J. S. *J. Chem. Phys.* **1984**, *80*, 3265−3269.
(100) Aquilante, F.; De Vico, L.; Ferré, N.; Ghigo, G.; Malmqvist, P.-Å.; Pedersen, T.; Pitonak, M.; Reiher, M.; Roos, B. O.; Serrano-Andrés, L.; Urban, M.; Veryazov, V.; Lindh, R. *J. Comput. Chem.* **2010**, *31*, 224−247.
(101) Frisch, M. J.; Trucks, G. W.; Schlegel, H. B.; Scuseria, G. E.; Robb, M. A.; Cheeseman, J. R.; Scalmani, G.; Barone, V.; Mennucci, B.; Petersson, G. A.; Nakatsuji, H.; Caricato, M.; Li, X.; Hratchian, H. P.; Izmaylov, A. F.; Bloino, J.; Zheng, G.; Sonnenberg, J. L.; Hada, M.; Ehara, M.; Toyota, K.; Fukuda, R.; Hasegawa, J.; Ishida, M.; Nakajima, T.; Honda, Y.; Kitao, O.; Nakai, H.; Vreven, T.; Montgomery, J. A.; Peralta, J. E.; Ogliaro, F.; Bearpark, M.; Heyd, J. J.; Brothers, E.; Kudin, K. N.; Staroverov, V. N.; Kobayashi, R.; Normand, J.; Raghavachari, K.; Rendell, A.; Burant, J. C.; Iyengar, S. S.; Tomasi, J.; Cossi, M.; Rega, N.; Millam, J. M.; Klene, M.; Knox, J. E.; Cross, J. B.; Bakken, V.; Adamo, C.; Jaramillo, J.; Gomperts, R.; Stratmann, R. E.; Yazyev, O.; Austin, A. J.; Cammi, R.; Pomelli, C.; Ochterski, J. W.; Martin, R. L.; Morokuma, K.; Zakrzewski, V. G.; Voth, G. A.; Salvador, P.; Dannenberg, J. J.; Dapprich, S.; Daniels, A. D.; Farkas, Ö.; Foresman, J. B.; Ortiz, J. V.; Cioslowski, J.; Fox, D. J. *Gaussian 09, Revision A.02*; Gaussian, Inc.: Wallingford, CT, 2010.
(102) Dunning, T. H. *J. Chem. Phys.* **1989**, *90*, 1007−1023.
(103) Kendall, R. A.; Dunning, T. H.; Harrison, R. J. *J. Chem. Phys.* **1992**, *96*, 6796−6806.
(104) Balabanov, N. B.; Peterson, K. A. *J. Chem. Phys.* **2005**, *123*.
(105) Roos, B. O.; Lindh, R.; Malmqvist, P. A.; Veryazov, V.; Widmark, P. O. *J. Phys. Chem. A* **2004**, *108*, 2851−2858.
(106) Roos, B. O.; Lindh, R.; Malmqvist, P. A.; Veryazov, V.; Widmark, P. O. *J. Phys. Chem. A* **2005**, *109*, 6575−6579.
(107) Forsberg, N.; Malmqvist, P.-Å. *Chem. Phys. Lett.* **1997**, *274*, 196−204.
(108) Ghigo, G.; Roos, B. O.; Malmqvist, P. A. *Chem. Phys. Lett.* **2004**, *396*, 142−149.
(109) Ruiperez, F.; Aquilante, F.; Ugalde, J. M.; Infante, I. *J. Chem. Theory Comput.* **2011**, *7*, 1640−1646.
(110) Gáspár, R. *Acta Phys. Acad. Sci. Hung.* **1974**, *35*, 213−218.
(111) Slater, J. C. *Phys. Rev.* **1951**, *81*, 385−390.
(112) Vosko, S. H.; Wilk, L.; Nusair, M. *Can. J. Phys.* **1980**, *58*, 1200−1211.
(113) Becke, A. D. *Phys. Rev. A* **1988**, *38*, 3098−3100.
(114) Perdew, J. P.; Burke, K.; Ernzerhof, M. *Phys. Rev. Lett.* **1996**, *77*, 3865−3868.
(115) Seeger, R.; Pople, J. A. *J. Chem. Phys.* **1977**, *66*, 3045−3050.
(116) Bauernschmitt, R.; Ahlrichs, R. *J. Chem. Phys.* **1996**, *104*, 9047−9052.
(117) Starcke, J. H.; Wormit, M.; Schirmer, J.; Dreuw, A. *Chem. Phys.* **2006**, *329*, 39−49.
(118) Levy, M. *Phys. Rev. A* **1982**, *26*, 1200−1208.
(119) Lieb, E. H. *Int. J. Quantum Chem.* **1983**, *24*, 243−277.
(120) Morrison, R. C. *J. Chem. Phys.* **2002**, *117*, 10506−10511.
(121) Kraisler, E.; Makov, G.; Argaman, N.; Kelson, I. *Phys. Rev. A* **2009**, *80*.
(122) Chai, J. D. *J. Chem. Phys.* **2012**, *136*, 154104.
(123) Kramida, A.; Martin, W. C. *J. Phys. Chem. Ref. Data*, **1997**, *26*, 1185−1194.
(124) Moore, C. E. *CRC Series in Evaluated Data in Atomic Physics*; Gallager, J. W., Ed.; CRC Press: Boca Raton, FL, 1993.
(125) Martin, W. C.; Kaufman, V.; Musgrove, A. *J. Phys. Chem. Ref. Data* **1993**, *22*, 1179−1212.
(126) Sugar, J.; Corliss, C. *J. Phys. Chem. Ref. Data* **1985**, *14* (Suppl. 2), 1−664.
(127) Sugar, J.; Musgrove, A. *J. Phys. Chem. Ref. Data* **1988**, *17*, 155−239.
(128) Moore, C. E. *Reference Data Series 35*, Vol. *III*; Gallager, J. W., Ed.; National Bureau of Standards: Washington, DC, 1971; p 245. (Reprint of NBS Circular 467, Vol. III, 1958.)
(129) Kramida, A.; Martin, W. C. *J. Phys. Chem. Ref. Data* **1997**, *26*, 1185−1194.
(130) Nielsen, E. S.; Jorgensen, P.; Oddershede, J. *J. Chem. Phys.* **1980**, *73*, 6238.
(131) Doering, J. P.; McDiarmid, R. *J. Chem. Phys.* **1980**, *73*, 3617.
(132) Bolovinos, A.; Tsekeris, P.; Anditopoulos, G. *J. Mol. Spectrosc.* **1984**, *103*, 240.
(133) Frueholz, R. D.; Flicker, W. M.; Mosher, O. A.; Kuppermann, A. *J. Chem. Phys.* **1979**, *70*, 2003.
(134) McDiarmid, R.; Sabjić, A.; Doering, J. P. *J. Phys. Chem. Ref. Data* **1985**, *83*, 2147.
(135) Wiberg, K. B.; de Oliveira, A. E.; Trucks, G. *J. Phys. Chem. A* **2002**, *106*, 4192−4199.
(136) Huber, K. P.; Herzberg, G. *Molecular Spectra and Molecular Structure: Constants of Diatomic Molecules*; Van Nostrand Reinhold: New York, 1979.
(137) Lofthus, A.; Krupenie, P. H.; Trucks, G. *J. Phys. Chem. Ref. Data* **1977**, *6*, 113.
(138) Bytautas, L.; Ruedenberg, K. *J. Chem. Phys.* **2005**, *122*, 154110.
(139) Casey, S. M.; Leopold, D. G. *J. Phys. Chem.* **1993**, *97*, 816.
(140) Vasiliu, M.; Feller, D.; Gole, J. L.; Dixon, D. A. *J. Phys. Chem. A* **2010**, *114*, 9349−9358.
(141) Jiang, W.; De Yonker, N. J.; Determan, J. J.; Wilson, A. K. *J. Phys. Chem. A* **2011**, *116*, 870−885.
(142) Zhang, W.; Truhlar, D. G.; Tang, M. *J. Chem. Theory Comput.* **2013**, *9*, 3965−3977.

NOTE ADDED AFTER ASAP PUBLICATION

This paper was published on the Web on August 5, 2014 with errors in the Abstract text and in eq 11. The corrected version was reposted on August 6, 2014.